Dual Projected Background Nulling Compressed Sensing for Robust Separation of Dynamic Contrast-Enhanced Angiograms

Suhyung Park[1], Eung Yeop Kim[2], and Jaeseok Park[3]

[1]Center for Neuroscience Imaging Research, Institute for Basic Science (IBS), Sungkyunkwan University, Suwon, Gyeong Gi-Do, Korea, [2]Department of Radiology, Gachon University Gil Medical Center, Incheon, Korea, [3]Biomedical Imaging and Engineering Lab., Department of Global Biomedical Engineering, Sungkyunkwan University, Suwon, Gyeong Gi-Do, Korea

Introduction: Dynamic contrast-enhanced magnetic resonance angiography (DCE-MRA) requires high spatiotemporal resolution, and typically employs subtraction between static reference and dynamic images followed by maximum intensity projection (MIP) to visualize time-varying angiograms[1,2] . Nevertheless, the subtraction-based DCE-MRA suffers from incomplete suppression of background signals in the presence of motion-induced voxel misregistration, potentially impairing the detectability of small distal vessels. In this work, we propose a novel reconstruction framework, dual projected background nulling compressed sensing (BANC), for robust separation of dynamic contrast-enhanced angiograms, in which we decompose x-t images into background static tissue signals (low rank component), background motion-induced signals (sparse component I), and DCE angiograms of interest (sparse component II) and then jointly estimate them while selectively nulling multiple background signals. Simulations and experiments validate that the proposed method is, if compared with conventional methods, highly effective in generating dynamic angiograms with robust background suppression even at very high reduction factors (R~30).

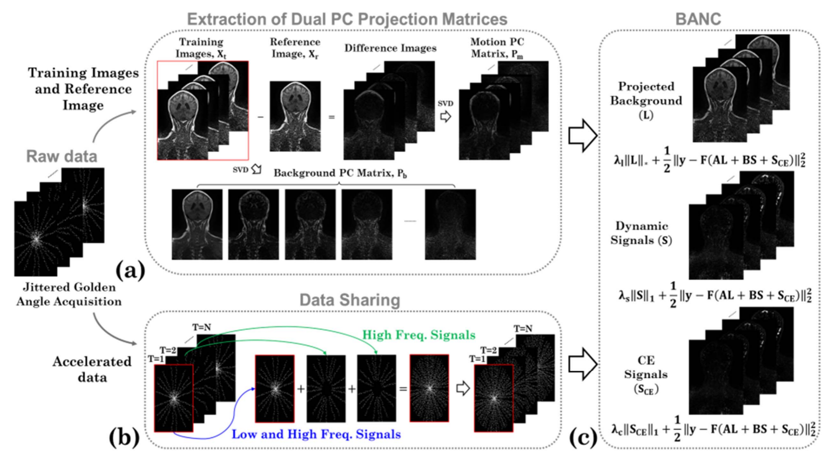

Figure 1. *Illustration of (a) construction of dual PC projection matrices, (b) data sharing, and (c) BANC reconstruction.*

Theory: 1) Signal Model: We decompose x-t images into linear superposition of background static tissue signals ($\mathbf{L}$, low rank component), background motion-induced signals ($\mathbf{S_m}$, sparse component I), and DCE angiograms of interest ($\mathbf{S_{CE}}$, sparse component II): $\mathbf{X} = \mathbf{L} + \mathbf{S_m} + \mathbf{S_{CE}}$ **(1)**. $\mathbf{S_m}$ represents motion-induced voxel misalignment between the reference (pre-contrast) and the DCE images (post-contrast). **2) Dual Projected BANC:** We construct the dual projection (principal coefficient) matrices for background static tissue signals and background motion-induced signals, respectively, by exploiting the reference image ($\mathbf{x_r}$) and the training data ($\mathbf{X_t} = [\mathbf{x_{t,1}}, \cdots, \mathbf{x_{t,n}}]$ contain background signals similar to actual dynamic images except for CE arteries and veins): $\mathbf{svd}(\mathbf{X_t}) = \mathbf{P_b \Sigma_b V_b^H}$ **(2)**, $\mathbf{svd}([\mathbf{x_{t,1}} - \mathbf{x_r}, \cdots, \mathbf{x_{t,n}} - \mathbf{x_r}]) = \mathbf{P_m \Sigma_m V_m^H}$ **(3)**, where $\mathbf{P_b}$ and $\mathbf{P_m}$ are the projection matrices for background static tissue and motion-induced signals, respectively. Then, to separate the dual background signals ($\mathbf{L}$, $\mathbf{S_m}$) from the DCE signals of interest ($\mathbf{S_{CE}}$), x-t images are projected onto the subspaces spanned by the dual projection matrices: $\mathbf{L} = \mathbf{P_b P_b' X}$ **(4)**; $\mathbf{S_m} = \mathbf{P_m P_m' S}$ **(5)** where $\mathbf{S} = \mathbf{S_m} + \mathbf{S_{CE}}$. Given the considerations above, Eq. (1) is rewritten by: $\mathbf{X} = \mathbf{P_b P_b' X} + \mathbf{P_m P_m' S} + \mathbf{S_{CE}} \Rightarrow \mathbf{X} = \mathbf{AL} + \mathbf{BS} + \mathbf{S_{CE}}$ **(6)** where $\mathbf{X} = \mathbf{L} + \mathbf{S}$, $\mathbf{A} = \mathbf{P_b P_b'}$, $\mathbf{B} = \mathbf{P_b P_b'} + \mathbf{P_m P_m'}$. Exploiting the suggested signal model, we proposed a novel, dual projected BANC reconstruction of DCE angiograms that jointly estimates $\mathbf{L}$, $\mathbf{S}$, and $\mathbf{S_{CE}}$:

P0: $\mathbf{arg\ min}_{\mathbf{L,S,S_{CE}}} \|\mathbf{L}\|_* + \boldsymbol{\lambda}_\mathbf{m}\|\boldsymbol{\varphi}(\mathbf{S})\|_1 + \boldsymbol{\lambda}_\mathbf{c}\|\boldsymbol{\varphi}(\mathbf{S_{CE}})\|_1$, s.t. $\mathbf{y} = \mathbf{F_u}(\mathbf{AL} + \mathbf{BS} + \mathbf{S_{CE}})$ **(7)** where $\boldsymbol{\lambda}_\mathbf{m}$ and $\boldsymbol{\lambda}_\mathbf{c}$ are the balancing parameters for background motion-induced signals and DCE signals of interest as compared to background static tissue signals, respectively, $\boldsymbol{\varphi}(\cdot)$ is an arbitrary prior to promote sparsity, $\mathbf{F_u}$ is the undersampled Fourier transform, and $\mathbf{y}$ is the measured k-space.

3) Sampling Pattern: To secure incoherent Fourier basis, we employ jittered golden-angle radial-like acquisition on the nearest Cartesian grid, wherein consecutive radial profiles are separated 111.25^{o} by adding a small amount of positional jitters. Additionally, view sharing is utilized by including the acquired data of the current frame while sharing the outer k-space with neighboring frames in a sliding block-wise fashion. An overall schematic of the proposed method is shown in Fig. 1.

Methods and Results: To validate the proposed method, in vivo brain data (320x240x144x20) in the k-t domain were acquired on a 3T clinical scanner. Fig. 2 represents the effective decomposition of the dual sparse components, $\mathbf{S_m}$ and $\mathbf{S_{CE}}$, from $\mathbf{S}$ during MIP (R = 1). Thus, the proposed, dual projected BANC eliminates residual background signals nearly completely, delineating vessels much more clearly than conventional subtraction-based methods (Fig. 3). Even with R ~ 30, the proposed dual projected BANC shows superior performance to CS with subtraction sparsity[3] in delineating angiograms (Fig. 4).

Conclusion: We demonstrated the effectiveness of the proposed, dual projected BANC for robust separation of DCE angiograms, effectively decoupling background sparse signals from sparse DCE signals of interest. Simulations and experiments reveal that the proposed method is highly competitive and outperforms against the existing methods. **References:** 1. Douek et. al., AJR, 165:431-437, 2. Wang et. al., MRM, 36:551-556, 3. Trzasko et. al., MRM 66:1019-1032.

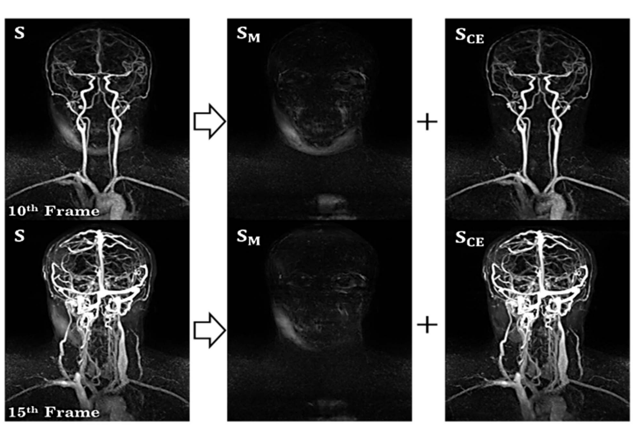

Figure 2. *Decomposition of* $\mathbf{S_m} + \mathbf{S_{CE}}$ *from dynamic sparse components (R=1)*

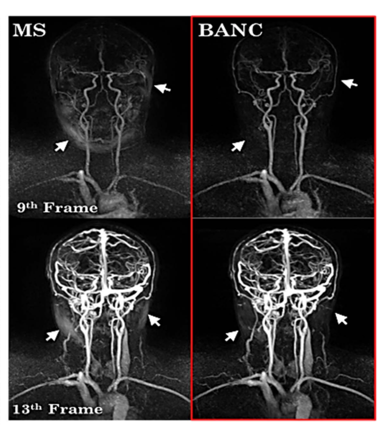

Figure 3. *Comparisons with magnitude subtraction (MS) vs. BANC (R=1)*

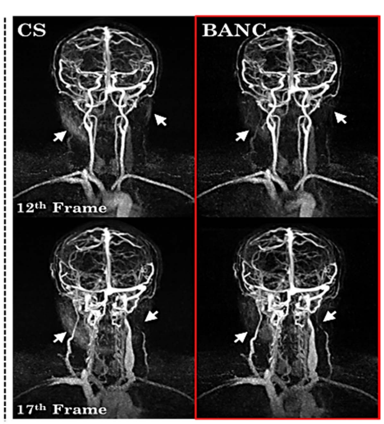

Figure 4. *Comparisons with compressed sensing (CS) vs. BANC (R~30)*